ELSEVIER

Thermochimica Acta 346 (2000) 63–72

thermochimica acta

www.elsevier.com/locate/tca

Dehydration and dehydroxylation of nontronites and ferruginous smectite

Ray L. Frost[a,*], Huada Ruan[a], J. Theo Kloprogge[a], W.P. Gates[b]

[a]*Centre for Instrumental and Developmental Chemistry, Queensland University of Technology, 2 George Street, GPO Box 2434, Brisbane Qld 4001, Australia*

[b]*CSIRO Land and Water, Private Mail Box 2, Adelaide, SA, Australia*

Received 3 May 1999; received in revised form 27 September 1999; accepted 28 September 1999

Abstract

Differential thermal analysis and thermogravimetry have been used to compare the dehydration and dehydroxylation behaviour of a series of nontronites including two newly discovered nontronites from Uley, South Australia. A comparison is made with the thermal behaviour of ferruginous smectite. Three dehydration endotherms were found at around 60°C, 100°C and 160°C. A strong dehydroxylation endotherm for all samples was found at ~430°C. The nontronites from Hohen-Hagen and Garfield show well-defined steps for dehydroxylation whereas the two Uley nontronites showed continuous dehydroxylation. The intensities of the infrared spectra of the hydroxyl-stretching region showed excellent correlation with the nontronite dehydroxylation endotherms. The infrared spectra of the water bending region showed two bands centred at ~1630 and 1670 cm^{-1}. These bands are attributed to adsorbed water and coordinated water.

Keywords: Differential thermal analysis; Differential thermogravimetry; Infrared absorption spectroscopy; Montmorillonite; Nontronite; Smectite

1. Introduction

Smectites belong to the group of hydrous clay minerals, which expand upon contact with water and other solvents [1,2]. Smectites may be either dioctahedral or trioctahedral structural types [3–5]. The dioctahedral smectites can be divided into two principal groups: (a) aluminium smectites and (b) the iron-rich varieties including ferruginous smectites and nontronites [4–6]. The ideal structural formula for aluminium smectites with octahedral charge (montmorillonites) is $X^{+}_{0.85}(Al_{3.15}Mg_{0.85})(Si_{8.0})O_{20}(OH)_4$, where X is a monovalent cation that counterbalances the layer charge [1]. In dioctahedral smectites, one of every three octahedral positions is vacant and the trivalent cations in the two filled sites typically share two hydroxyl (OH) ligands. Smectites contain both adsorbed and structural water [1]. Both the Al and Mg occupy the octahedral sheet. Two types of dioctahedral smectites exist depending on the site of the layer charges: (a) montmorillonites where the charge arises from divalent cations, usually Mg, which substitutes for Al in the octahedral sites, (b) beidellites where the charge arises from the aluminium substitution for

* Corresponding author. Tel.: +61-7-3864-2407; fax: +61-7-3864-1804.

E-mail address: r.frost@qut.edu.au (R.L. Frost).

0040-6031/00/$ – see front matter
PII: S0040-6031(99)00366-4

silicon in the tetrahedral sites. Ferruginous smectites have partial substitution of the aluminium by iron. In nontronites almost all of the Al in the octahedral layer is replaced with ferric iron (Fe^{3+}). In this case the structural formula is given by $(M_x^+ nH_2O)(Fe_4^{3+})(Si_{4x}Al_x)O_{20}(OH)_4$. This clay is the end member and is known as nontronite [5–6]. Montmorillonites and beidellites have $Fe^{3+} < 1$ mol%. The term nontronite is used for dioctahedral smectites when Fe^{3+} is >3 mol% and when the layer charge originates from the tretrahedral sheet.

Two nontronites from Garfield (Spokane County, Washington, USA) and Hohen-Hagen (Germany) have been extensively used as reference clays [7] but are becoming very difficult to obtain. Recently, two nontronites were discovered at the Uley Graphite mine near Port Lincoln, South Australia, within heavily weathered granulite facies schist, gneiss and amphibolite of Palaeoproterozoic age. Geologic evidence indicates two distinct nontronites are present: a green nontronite associated with weathered biotite schist bands, and a brown nontronite filling joints and fractures within the amphibolite composed of anorthite and highly altered alumino-ferro-hornblende [8]. Preliminary mineralogical and chemical analyses support this finding and indicate that the Uley green nontronite is similar in chemistry and structure to the Garfield nontronite, whereas the Uley brown nontronite appears to be significantly lower in aluminium and possibly contains tetrahedrally coordinated iron.

Thermal analysis of clay minerals can provide valuable information about the chemical composition of clay minerals [8], particularly in the lower temperature regime (<700°C). The study of the dehydroxylation of smectites can be complicated by a nearly continuous evolution of water at temperatures below about 400°C [9]. These waters include surface-sorbed waters of hydration and coordination waters of interlayer cations. In addition, the dehydroxylation event often occurs over a range of temperatures [10]. For the aluminium-enriched smectites, the loss of hydroxyls typically commences at temperatures >700°C, however, for the iron-enriched smectites, the temperatures at which dehydroxylates are formed are often as low as 450°C. Thus significant overlap can occur between dehydration and dehydroxylation of ferruginous smectites. For nontronites, these reactions are further complicated by the formation of ancillary phases: maghemite when heated under air or argon and fayalite when heated under H_2/N_2 [8]. The aim of this paper is to describe the thermal decomposition of nontronites, including the Uley nontronites and a ferruginous smectite in terms of dehydration and dehydroxylation and to utilise thermal techniques to further understand the similarities and differences between the two Uley nontronites with each other and with reference nontronites. The two Uley nontronites have been submitted to the Clay Minerals Repository of The Clay Minerals Society and portions are available for research.

2. Materials and methods

2.1. Clay minerals

The clay minerals used are the Clay Mineral Society standards: the ferruginous smectite SWa-1, the Garfield nontronite from Spokane County, Washington, USA labelled as API-H33a, or sometimes H33a [5], and the nontronite NG-1 from Hohen-Hagen, Germany [7]. The two Australian samples are from Uley Graphite Mine, Eyre Peninsula, South Australia. The calcium exchanged, <1 μm portions were used. Samples were analysed for purity by X-ray diffraction. Infrared spectroscopy was also used to detect low levels of other phases, particularly kaolinite and amorphous phases. The Uley green nontronite (NAu-1) sample contained traces of kaolinite and the Uley brown nontronite (NAu-2) contained calcite and ferrihydrite. The contaminants were at very low levels and were not detected by XRD. Both the Uley nontronites are now available from the Source Clay Minerals Repository at the University of Missouri.

The ferruginous smectite SWa-1 from the Clay Mineral Repository (Grant County, Washington) has a structural formula of $(M_{0.95}^+)[Al_{1.10}Fe_{2.61}Mg_{0.25}][Si_{7.40}Al_{0.60}]O_{20}(OH)_4$. The nontronite from Hohen-Hagen, Germany (CMR NG-1) has a structural formula of $(M_{0.95}^+)[Al_{0.86}Fe_{3.08}Mg_{0.05}][Si_{7.12}Al_{0.11-0.11}Fe_{0.76}]O_{20}(OH)_4$.It should be noted that titanium as anatase occurs as an admixture in this nontronite and some of the Fe (≈20%) is in the tetrahedral layers. The Garfield nontronite from Spokane County, Washington, has a formula $(M_{1.07}^+)[Al_{0.23}Fe_{3.71}Mg_{0.03}]_{0.03}][Si_{7.03}Al_{0.97}]O_{20}(OH)_4$. It should be noted that

there is another nontronite from Spokane, Washington County, titled Spokane nontronite. This is an extremely rare mineral and was not used in this work. The Uley Green (NAu-1) nontronite has a formula of $[M^{+}_{1.05}][Al_{0.26}Fe_{3.71}Mg_{0.03}][Si_{6.97}Al_{1.03}]O_{20}(OH)_4$ and the Uley brown (NAu-2) nontronite has a formula of $[M^{+}_{0.83}]$ $[Al_{0.42}Fe_{3.43}Mg_{0.04}]$ $[Si_{7.52}Al_{0.06}Fe_{0.42}]$ $O_{20}(OH)_4$. Nontronites contain Fe predominantly in the trivalent state [5,8,10]. The above analyses were conducted on ignited, Ca-saturated purified fractions (nominally <0.15 μm) of each nontronite.

The minerals were selected to provide a range of total Fe^{3+} and Al contents. The Fe content (ignited, Fe_2O_3 basis) are: for SWa-1, 24.4%; Uley green 36.49; Garfield 36.4; Ng-1, 37.5%; Uley brown 38.1. The aluminium content of SWa-1 11.04%, for the Garfield nontronite 7.54% and NG-1 nontronite 6.06%. The aluminium content of the Uley green nontronite is 8.15% and of the brown sample 3.02%. It should be noted that NG-1 and the Uley brown nontronite each contains significant amounts of ferric iron in the tetrahedral sheet. However each of the nontronites studied here contain most of the iron as ferric iron in the octahedral sheet. The SWa-1 is usually referred to as a ferruginous smectite rather than a nontronite due to its elevated Mg content, low tetrahedral Al substitution and high proportionate charge residing in the octahedral layer. Thus, based on chemical composition, the Uley smectites are members of the smectite series in which the octahedral aluminium has been replaced by octahedral ferric iron.

2.2. Infrared absorption spectroscopy

Absorption spectra were obtained using a Perkin-Elmer Fourier transform infrared spectrometer (2000) equipped with a TGS detector. Spectra were recorded by accumulating 1024 scans at 4 cm^{-1} resolution and a mirror velocity of 0.3 cm/s in the mid-IR. Spectral manipulation such as baseline adjustment, smoothing and normalisation was performed using the Spectracalc software package GRAMS (Galactic Industries Corporation, NH, USA). Band component analysis was undertaken using the Jandel 'Peakfit' software package which enabled the type of fitting function to be selected and allows specific parameters to be fixed or varied accordingly. Band fitting was done using a Lorentz–Gauss cross-product function with the minimum number of component bands used for the fitting process. The Gauss–Lorentz ratio was maintained at values greater than 0.7 and fitting was undertaken until reproducible results were obtained with squared correlations of $r^2 > 0.99$. Graphics are presented using Microsoft excel.

2.3. DTA/TGA

Differential thermal and thermogravimetric analysis on ~50 mg of the size fractioned smectite minerals was obtained using a Setaram DTA/TGA instrument, operating at 0.5°C/min from ambient temperatures to 1000°C in a nitrogen atmosphere. The fact that the DTA experiment is conducted in an inert atmosphere means that the samples cannot oxidise during thermal treatment.

3. Results and discussion

3.1. Dehydration

The TGA, differential thermogravimetric and DTA patterns for the two reference nontronites, Garfield and NG-1, and the two Uley nontronites together with the ferruginous smectite are shown in Fig. 1(i) and (ii) and Fig. 2. The percentage weight losses of the dehydration and dehydroxylation steps are reported in Table 1. The analyses of the DTA patterns are reported in Table 2. In both the TGA and DTA patterns, a lot of commonality exists in the suite of samples. Weight losses occur between 100°C and 120°C and over the temperature range 400–500°C. All samples lost weight between 60°C and 100°C and some of the nontronites between 120°C and 160°C. This weight loss represents the dehydration of the minerals [11–13]. The second weight loss region occurs over the 400–500°C temperature range and represents the dehydroxylation of the clays.

The weight loss is represented by changes in the TGA patterns (Fig. 1(i)). Three dehydration steps are observed and one principle dehydroxylation step. Such steps are more readily observed in the DTGA plots in Fig. 1(ii). The bulk of the water is lost in the first dehydration step, which occurs over the 60–120°C temperature range. The wt.% loss varies between samples but is between 12.1 and

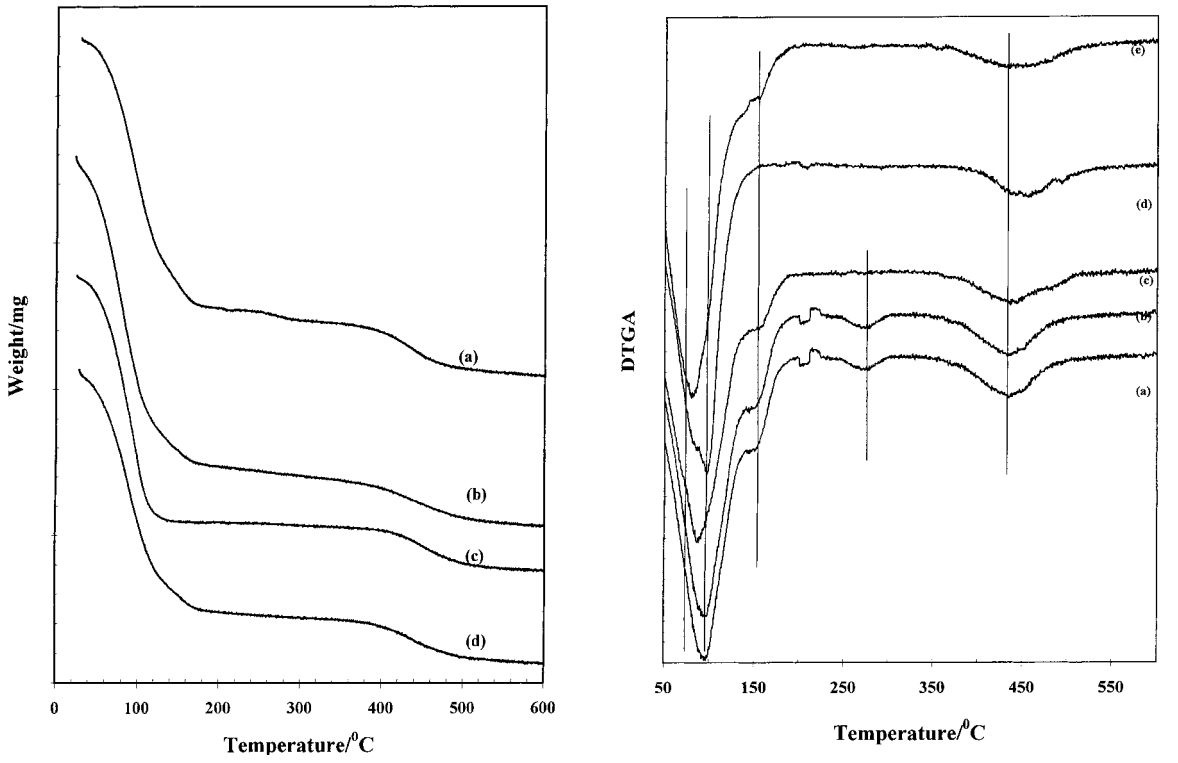

Fig. 1. (i) Thermogravimetric analysis of: (a) ferruginous smectite; (b) Hohen-Hagen nontronite; (c) Uley nontronite (brown); (d) Uley nontronite (green). (ii) Differential thermogravimetric analysis of: (a) ferruginous smectite; (b) Hohen-Hagen nontronite; (c) Uley nontronite (brown); (d) Uley nontronite (green).

15.0 wt.%. The second dehydration step starts at ~120°C and is complete by 160°C, and the weight change varies between 2.5 and 4 wt.%. The third dehydration step is ~160°C and a loss of around 1% is observed. For the Uley brown nontronite, only one dehydration step could be observed. A small weight loss of 0.90% is observed over the 200–300°C temperature range. This small weight loss is quite often observed for smectites and may be attributed to the overlap of the dehydration and dehydroxylation steps.

The results presented here are in agreement with previously published data [8]. Greater weight losses are observed in this work and we have differentiated steps in the dehydration process. The weight loss during the dehydroxylation step is around 4% and is consistent for all samples. The theoretical weight loss of the dehydroxylation step for a nontronite is

Table 1
Percentage weight losses during dehydration and dehydroxylation of nontronites and ferruginous smectite

Clay mineral	Dehydration 1 (wt.%)	Dehydration 2 (wt.%)	Dehydration 3 (wt.%)	Dehydroxylation 1 (wt.%)
Temperature range	25–90°C	90–110°C	110–160°C	400–450°C
Nontronite Hohen-Hagen	12.1	4.0	1.3	3.6
Nontronite Garfield	13.9	2.5	1.3	4.0
Ferruginous smectite	15.0	3.6	0.9	3.6
Uley (green)	12.7	2.5	2.3	4.0
Uley (brown)	16.6			3.9

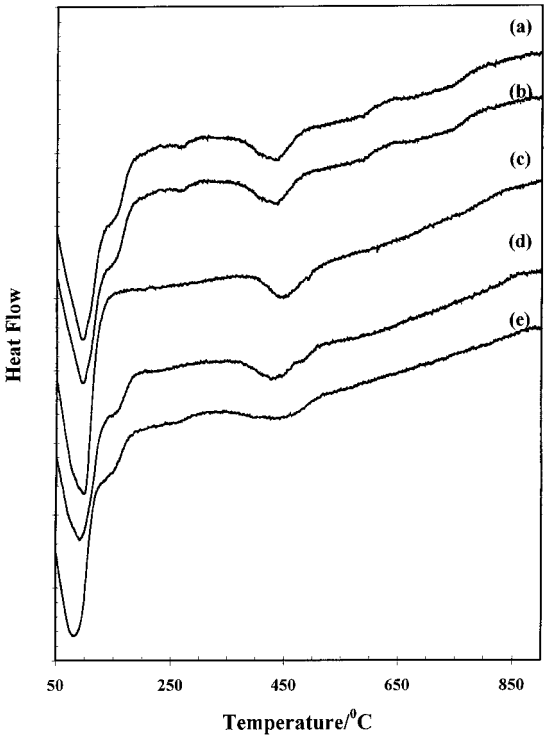

Fig. 2. Differential thermal analysis of: (a) Hohen-Hagen nontronite; (b) Uley nontronite (brown); (c) Uley nontronite (green); (d) Garfield nontronite; (e) ferruginous smectite.

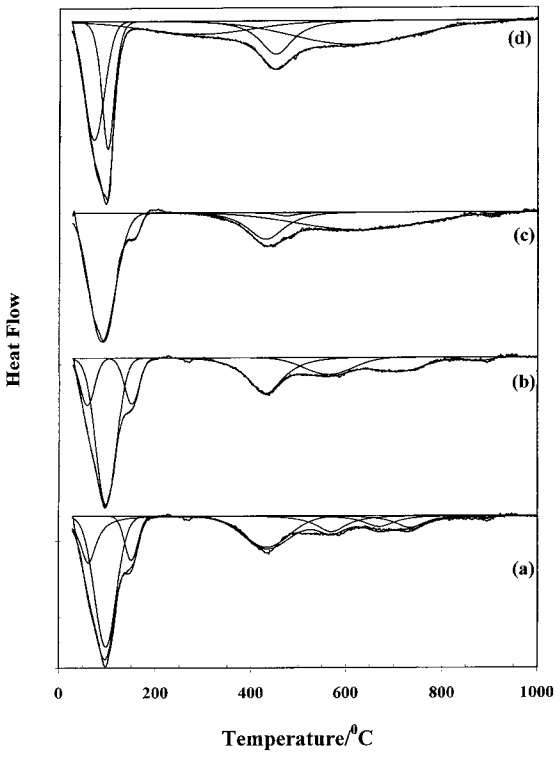

Fig. 3. Band component analysis of the DTA pattern of: (a) Hohen-Hagen nontronite; (b) Garfield nontronite; (c) Uley green nontronite; (d) Uley brown nontronite.

3.96%. Thus the experimentally observed dehydroxylation weight loss values for the two Uley nontronites are close to the theoretical value and agree with published values [9]. The TGA patterns show that the thermal behaviour of the two South Australian nontronites closely follow the behaviour of the more well-known nontronites from Hohen-Hagen and Garfield, thus making the South Australian nontronites most suitable as replacement clay mineral standards.

The DTA patterns (Fig. 2) of all samples show similar features with a complex dehydration endotherm and a dehydroxylation endotherm centred on 450°C. Fig. 3 shows the component analysis of the endotherms for the two standard nontronites from Hohen-Hagen and Garfield together with those of the Uley nontronites. The first three endotherms are observed for both reference nontronites at 62°C, 97°C and 151°C and are attributed to the loss of adsorbed water (62°C and 97°C) and the loss of coordinated water (151°C). For the Hohen-Hagen nontronite, 12.9% of the total energy of dehydration and dehydroxylation is utilised at 62°C and is attributed to the energy required to remove the adsorbed water and 38% of the total energy is utilised at 97°C and is attributed to water of hydration of the cation (Table 2). These values for the Garfield nontronite are 6.0% and 28.0%. The ferruginous smectite showed two water desorption endotherms at 60°C and 91°C with 17.7% and 28.0% relative areas (Fig. 3c). Such thermal values are not unexpected as smectites containing hydrated cations contain large amounts of water. The Uley green nontronite did not show the low temperature endotherm at ~60°C. However, a large water desorption endotherm at 89°C was observed with a relative area of 47% (Fig. 3d). The Uley brown nontronite showed desorption isotherms at 72°C and 100°C with 14.9% and 10.9% relative thermal energies (Fig. 3e). The difference in thermal energies for the water adsorption between the two Uley nontronites suggests differences in chemical structure. This is also

Table 2
Component analysis of the thermal energy ratios of nontronites and ferruginous smectites

Clay mineral	Endo 1	Endo 2	Endo 3	Endo 4	Endo 5	Endo 6	Endo 7	Endo 8
Nontronite, Hohen-Hagen	62°C, 12.9%	97.0°C, 38.0%	151°C, 7.9%	433°C, 20.4%	567°C, 9.5%	670°C, 5.1%	735°C, 5.1%	889°C, 0.3%
Nontronite, Garfield	59°C, 6.0%	98°C, 28.4%	151°C, 6.3%	430°C, 27.6%	563°C, 16.0%		708°C, 13.1%	875°C, 1.2%
Ferruginous smectite	60°C, 17.7%	91°C, 28.0	144°C, 6.3%	440°C, 19.9%	606°C, 26.0%			961°C, 2.1%
Uley (green)		89°C, 47%	156°C, 3.0%	434°C, 18.0%	629°C, 31.4%			907°C, 0.3%
Uley (brown)	72°C, 14.9%	100°C, 10.9%	289°C, 18.3%	451°C, 17.5%	613°C, 38.5%			

exemplified by the cation water of hydration endotherms. The Uley green nontronite has an endotherm at 156°C that is 3.0% of the total thermal energy. The Uley brown nontronite shows no endotherm at ~150°C but does have a broad endotherm at 289°C with 18.3% of the total thermal energy. This broad endotherm is attributed to the presence of some ferrihydrite impurity in this nontronite. The low temperature thermal behaviour of the two Uley nontronites suggests that the two minerals are different, resulting from different diagenetic origins in agreement with the chemical and geological analyses.

Hydration in clay minerals is readily observed by studying the infrared spectrum of the water bending modes centred on 1630 cm^{-1}. This band has proven most sensitive to changes in the structural environment of the water [14–15]. Water, which is coordinated to cations in clays, occurs around 1680 cm^{-1}, water in the hydration sphere of cations around 1650 cm^{-1} and adsorbed water at 1630 cm^{-1}. The spectra of the water bending modes of the nontronites are illustrated in Fig. 4 and the band component analysis reported in Table 3. In Table 3 bands are labelled as v_1 starting from the highest frequency to v_x the lowest frequency. In Table 3, the HOH water bending vibration with the highest frequency is v_1 with a frequency of 1680 cm^{-1}. The bending mode with the lowest frequency is v_4 with a frequency of 1613 cm^{-1}. This labelling is according to normal spectroscopic convention. The water in the Hohen-Hagen nontronite shows two bands at 1680 and 1632 cm^{-1} with relative areas of 44.0% and 55.0%. The first band is attributed to water coordinated to the interlayer cation. The second band is attributed to adsorbed water. A similar feature is observed for the Garfield nontronite but the ratio of the two bands is now 19.5–80.5%. For the ferruginous smectites bands are observed at 1670 and 1635 cm^{-1} with relative intensities of 39.5% and 60.5%. The Uley green nontronite shows two bands at 1672 and 1635 cm^{-1} with relative areas of 23.3% and 58.0%. An additional band is observed at 1613 cm^{-1} and is attributed to weakly hydrogen bonded interlayer water. Such a band component analysis is typical of smectites. The water-bending region is different for the Uley brown nontronite. Two bands are observed at 1654 and 1630 cm^{-1} with relative areas of 21.9% and 78.1%. In the DTA pattern no endotherm was observed at ~150°C and the water band at ~1680 cm^{-1} is also not observed.

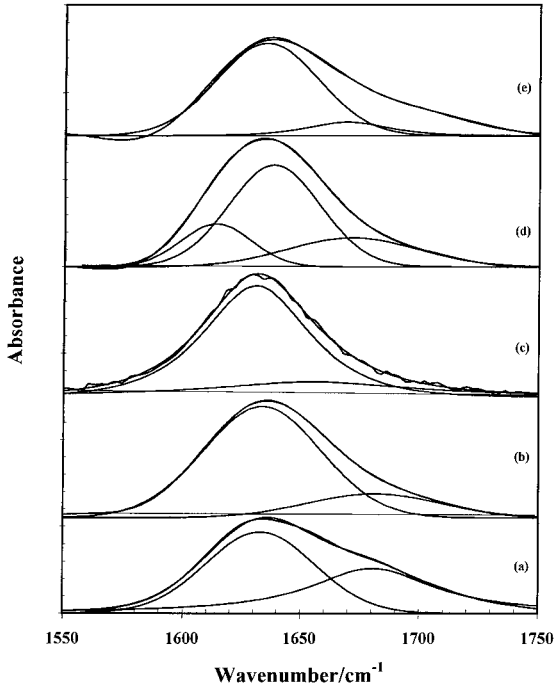

Fig. 4. Band component analysis of the infrared spectrum of the water bending mode for: (a) Hohen-Hagen nontronite; (b) Garfield nontronite; (c) Uley green nontronite; (d) Uley brown nontronite.

Table 3
Table of the water-bending region of the infrared absorption spectra of nontronites and ferruginous smectites

Band cm^{-1}/area	Nontronite Hohen-Hagen	Nontronite Garfield	Fe-smectite	Uley green	Uley brown
v_1	1680, 44.0%	1682, 19.5%	1670, 39.5%	1672, 23.3%	
v_2					1654, 21.9%
v_3	1632, 55.0%	1634, 80.5%	1635, 60.5%	1635, 58.0%	1630, 78.1%
v_4				1613, 18.7%	

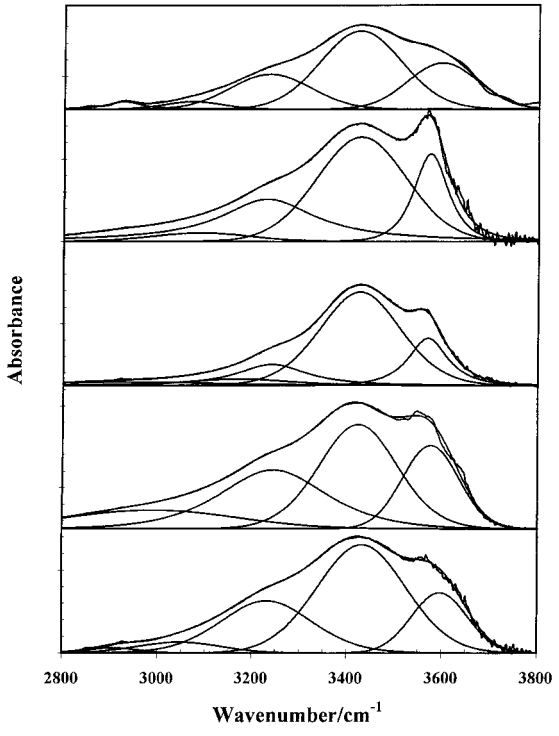

Fig. 5. Band component analysis of the infrared spectrum of the hydroxyl stretching region for: (a) Hohen-Hagen nontronite; (b) Garfield nontronite; (c) Uley green nontronite; (d) Uley brown nontronite.

The hydroxyl stretching region of the series of nontronites are shown in Fig. 5. The results of the band component analyses are reported in Table 4. This table reports the following common characteristics of the infrared spectra of nontronites are: (a) a peak in the 3570–3590 cm^{-1} region attributed to the hydroxyl stretching vibration of $Fe_2^{3+}OH$; (b) a broad band centred at 3430 cm^{-1} attributed to adsorbed water and (c) a band centred between 3230 and 3245 cm^{-1} ascribed to coordinated water. The relative intensity of the 3697 cm^{-1} band of Hohen-Hagen nontronite is 17.6%. The values of the two Uley nontronites are 16.4% and 17.0% and are close to the value for the first nontronite. The band for the ferruginous smectite is observed at 3597 cm^{-1} and has a relative intensity of 24.3% which is higher than for the other minerals. However here the bandwidth should be taken into account because of the significant Al–Fe–OH and Al–Al–OH bands in SWa-1. The bandwidth of the v_1 band for Hohen-Hagen nontronite, Garfield nontronite, green Uley nontronite and brown Uley nontronite are 137, 138, 83 and 96 cm^{-1}, whereas the bandwidth of the v_1 band for the ferruginous smectite is 175 cm^{-1}.

A good correlation exists between the intensities of the infrared bands and the weight losses in the TGA. Fig. 6 shows the weight loss during dehydration as a function of the intensity of the infrared absorption bands. Two groups of data are observed according to the 1630 and ~1670 cm^{-1} bands. The squared correlation coefficient of 0.91 is obtained. Such a result is excellent considering that the intensities of the infrared bands were determined by curve fitting. This data shows the relationship between a molecular property as measured by infrared absorption spectroscopy and the thermogravimetric analysis, which is measuring a bulk property. A similar relationship between the infrared absorption of the stretching frequencies could be expected. However because of the overlap of the water hydroxyl stretching vibrations with the Al–Fe^{3+} and Fe_2^{3+} hydroxyl stretching vibrations, such a correlation was not found.

3.2. Dehydroxylation

A sequence of dehydroxylation endotherms is observed at 433, 567, 670 and 735°C for the Hohen-Hagen nontronite (Table 2). The relative areas

Table 4
Table of the hydroxyl-stretching region of the infrared absorption spectra of nontronites and ferruginous smectites

Band cm^{-1}/area	Nontronite Hohen-Hagen	Nontronite Garfield	Fe-smectite	Uley green	Uley brown
v_1	3597, 17.6%	3576, 20.5%	3597, 24.3%	3569, 16.4%	3573, 17.0%
v_2	3432, 50.9%	3423, 36.7%	3424, 48.3%	3426, 59.2%	3427, 48.3%
v_3	3232, 25.5%	3245, 29.4%	3234, 21.4%	3241, 13.6%	3230, 28.1%
v_4	3048, 5.9%	3050, 13.3%	3070, 3.4%	3172, 10.6%	3090, 6.6%

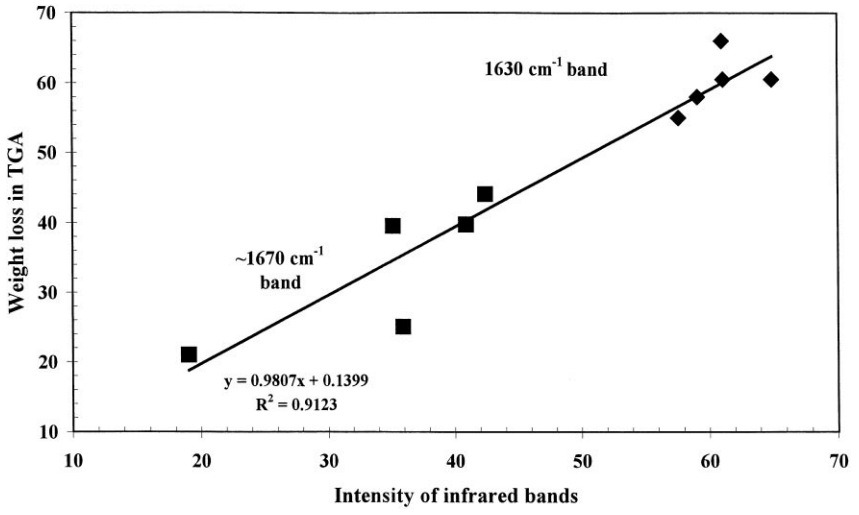

Fig. 6. Relationship between the intensity of the water bending modes and the weight loss in thermogravimetric analysis due to dehydration.

of these endotherms are 20.4%, 9.5%, 5.1% and 5.1%. The principal dehydroxylation temperature is 433°C. The series of endothermic steps suggests that the dehydroxylation of this nontronite is occurring in steps. For the Garfield nontronite, dehydroxylation endotherms were observed at 430°C, 563°C and 708°C with relative areas of 27.6%, 16.0% and 13.1%. A minor endotherm was observed for both the Hohen-Hagen and Garfield nontronites at ~880°C and is attributed to a phase change. Infrared emission spectroscopy of the low frequency region of these two nontronites shows a change in the infrared spectrum around this temperature. Thus a change in the molecular structure at 880°C supports the results of the DTA analyses. The dehydroxylation of the Garfield nontronite is similar to that of the Hohen-Hagen nontronite except that the third dehydroxylation step is not resolved. However, the last step in the dehydroxylation is broad thus there is likely little difference between the thermal evolution of these two nontronites. The ferruginous smectite shows two dehydroxylation steps similar to the Garfield nontronite with endotherms at 440°C and 606°C. The relative areas of these two endotherms are 19.9% and 26.0%. It is noteworthy that the relative areas of the two dehydroxylation steps of Garfield nontronite and the ferruginous smectite are reversed. (27.6% and 16.0% compared with 19.9% and 26.0%). The major difference between the two minerals is the amount of aluminium in the octahedral sheet. The ferruginous smectite contains more aluminium. Thus the two steps at ~430°C and 565°C are attributed to the dehydroxylation of firstly the OH associated with Fe–Fe pairs and secondly the OH associated with Fe–Al pairs [10]. The Uley green nontronite shows a sharp dehydroxylation endotherm at 434°C and a broad endotherm centred at 629°C. The relative areas of these two endotherms are 18.0% and 31.4%. These two endotherms for the Uley brown nontronite are observed at 451°C and 613°C with areas of 17.5% and 38.5%. Distinct steps of dehydroxylation were not resolvable for the Uley nontronites, as they were for the Hohen-Hagen nontronite and it can be concluded that the dehydroxylation of the Uley nontronites is occurring as a continuous process. The exact reasons for the difference in thermal behaviour of the two Uley nontronites compared to the reference nontronites are unclear. One possible reason for this could be the very small particle size of the two Uley nontronites. A second possibility is that these are not dehydroxylation steps but rather possible phase changes.

If a comparison is made between the areas of the DTA endotherm 4 and the areas of the ν_1 band, a good linear relationship is found except for the ferruginous smectite. Thus the amount of dehydroxylation of the hydroxyls associated with octahedral iron is directly

related to the intensity of the IR active v_1 band. A comparison between the area of endotherm 2 and the intensity of the v_2 band at $\sim$3430 cm^{-1} is also reasonably well correlated. This logically shows the v_2 band attributed to the hydroxyl stretching frequency of water results in the endotherm 2 of the DTA. This type of comparison between the areas of the endotherms and the intensity of the infrared bands is quite reasonable. While FTIR measures molecular properties and DTA is determining thermal-physical properties of water, both techniques are providing information on the bulk water associated with the smectites.

4. Conclusions

A combination of DTA/TGA and infrared spectroscopy has been used to study the dehydroxylation and dehydration of a series of nontronites including some newly discovered nontronites from Uley graphite mine, Eyre peninsula, South Australia. The spectral features of the nontronites are significantly different to that of the ferruginous smectite and the Uley nontronites may be compared with both the Garfield and Hohen-Hagen nontronites. The infrared spectra of the hydroxyl-stretching region of all the nontronites are similar but differ substantially from that of the ferruginous smectite. However, the dehydration and dehydroxylation behaviour of the ferruginous smectite and the three other nontronites are similar. The thermal decomposition of the brown Uley nontronite is different and apparently this difference may be attributed to the presence of a minor component of ferrihydrite in the clay.

Acknowledgements

The financial and infra-structure support of the Queensland University of Technology Centre for Instrumental and Developmental Chemistry is gratefully acknowledged. Mr S.C. Russell is thanked for undertaking the thermal analyses. The authors would like to thank J. Keeling and M. Raven for providing the Uley nontronites.

References

[1] R.E. Grim, G. Kulbicki, Am. Mineralogist 46 (1961) 1329.
[2] J. Wu, P.F. Low, C.B. Roth, Clays Clay Mineral. 37 (1989) 211.
[3] S. Petit, J.-L. Robert, A. Decarreau, G. Besson, O. Grauby, F. Martin, Bull. Cent. Rech. Explor.-Prod. Elf-Aquitaine 19 (1995) 119.
[4] O. Grauby, S. Petit, A. Decarreau, A. Baronnet, Eur. J. Mineral. 6 (1994) 99.
[5] A. Manceau, D. Chateigner, W.P. Gates, Phys. Chem. Mineral. 25 (1998) 347.
[6] P. Komadel, J. Madejova, J.W. Stucki, Clays Clay Mineral. 43 (1995) 105.
[7] P. Schneiderhorn, Tschermaks Min.u. Petr. Mitt. 10(1)–4 (1965) 386.
[8] K.J.D. Mackenzie, D.E. Rogers, Thermochim. Acta 18 (1977) 177.
[9] B.S. Girgis, K.A. El Baraway, N.S. Felix, Thermochim. Acta 111 (1987) 9.
[10] L. Heller-Kallai, I. Rozenson, Clays Clay Mineral. 28 (1980) 355.
[11] R.L. Frost, M. Vassallo, Clays Clay Mineral. 44 (1996) 635.
[12] R.L. Frost, S.M. Dutt, J. Colloid Interface Sci. 198 (1998) 330.
[13] R.L. Frost, J.T. Kloprogge, S.C. Russell, J.L. Szetu, Thermochim. Acta 329 (1999) 47–56.
[14] R.L. Frost, J. Kristof, G.N. Paroz, T.H.T. Tran, J.T. Kloprogge, J. Colloid Interface Sci. 204 (1998) 227.
[15] R.L. Frost, J. Kristof, G.N. Paroz, J.T. Kloprogge, J. Colloid Interface Sci. 208 (1998) 216.